Scientia Iranica B (2014) 21(3), 609–619

Sharif University of Technology
Scientia Iranica
Transactions B: Mechanical Engineering
www.scientiairanica.com

Prediction of all-steel CNG cylinder fracture under impact using a damage mechanics approach

M. Yazdani Ariatapeh, M. Mashayekhi* and S. Ziaei-Rad

Department of Mechanical Engineering, Isfahan University of Technology, Isfahan, P.O. Box 84156-83111, Iran.

Received 15 October 2012; received in revised form 5 August 2013; accepted 4 November 2013

KEYWORDS
All-steel CNG cylinder;
Damage mechanics;
Fracture;
Impact.

Abstract. In this paper, a damage mechanics approach is used to investigate the effect of crash and damage caused by impact in a steel cylinder filled by Compressed Natural Gas (CNG). The Canadian Standard Association (CSA) for CNG cylinders is used as a damage detection criterion, and the cylinders' capability of reuse. The Johnson-Cook damage model is used to compute cylinder failures. Simulations are carried out in different impact directions, and the effect of cylinder internal pressure, collision velocity and fall height are analyzed. Also, failure due to collisions in various situations is studied and discussed. Investigations for cases including crash and drop tests showed that the maximum damage in a cylinder is created in the case of normal impact and, by changing impact direction from normal to the side, the amount of damage will be decreased. Also, by eliminating failed elements and comparing the damage depth caused by collision using the CSA standard, it was observed that in most cases of normal accidents and drop tests, damaged cylinders lose their ability for reuse. However, in the case of side impact, the cylinder remains intact or can be reused after repair.

1. Introduction

High costs and the risk of empirical testing make the use of numerical methods inevitable. From an economical viewpoint, natural gas is frugal fuel, with low cost and abundant resources, and natural gas combustion pollution is lower than other common fossil fuels, such as gasoline and diesel. On the other hand, a major issue in the use of natural gas fuel in cars is the storage problem. Compressed natural gas cylinders are used for the storage of fuel at high pressure in cars with CNG. These cylinders are divided into four categories according to the manufacturer's material, including: all-metal, metal liner hoop wrapped, metal liner fully wrapped and all-composite. All-steel cylinders with about 92% percent usage are the most common type of cylinder and the history of these cylinders goes back to the 1970s. Safety is one of the important issues in the design and manufacture of such cylinders. All-metal cylinders use better known technology, with respect to the other types of cylinder and, therefore, have more safety performance capability. According to the importance of safety and to decrease the concerns of gas fuel car passengers, especially considering the effects of car accidents on CNG cylinders, it is necessary to investigate cylinder impact conditions before use. Despite this, almost no studies have been reported on the impact phenomenon of CNG cylinders. Some related studies have been quoted in the following paragraphs.

In 1991, Becker et al. mentioned that the reactor pressure vessel/neutron shield tank assembly could be shipped safely without any risk to the public or the environment [1]. The reactor pressure vessel/neutron

*. *Corresponding author. Tel.: +98 311 3915216; Fax: +98 311 3912628*
E-mail addresses: m.yazdaniariatape@me.iut.ac.ir (M. Yazdani Ariatapeh); mashayekhi@cc.iut.ac.ir (M. Mashayekhi); szrad@cc.iut.ac.ir (S. Ziaei-Rad)

shield tank assembly was certified by the U.S. Department of Energy as a type B package. A safety analysis report for packaging was prepared in accordance with the U.S. Department of Energy requirements to provide the technical basis for the U.S. Department of Energy certification. The reactor pressure vessel/neutron shield tank package is a monolithic structure of lightweight concrete and steel. To substantiate multidimensional inelastic analyses, a series of drop tests was conducted on several benchmark models from various heights. Technical evaluation and correlation of the test data were performed in conjunction with the structural analysis and assessment of the package. Their research provides a comprehensive discussion on the benchmark drop models and specific drop tests and also addresses the results obtained from comparing technical data with analytical data. The purpose of the benchmark tests was to demonstrate that the results of the structural analyses of the package are a reasonable representation of its real structural behavior.

In 1994, Rosenberg et al. conducted a series of experiments on high pressure vessels made of stainless steel in order to determine the critical pressures for catastrophic failure under projectile impact [2]. By using gas dynamics calculations based on an ideal gas equation of state expanding isothermally through a hole in the pressurized cylinder and adiabatic expansion of a non-ideal gas, they found that there is constant pressure within the vessel throughout the whole process. In 2006, Nagel and Thambiratnam compared the energy absorption response of straight and tapered thin-walled rectangular tubes under oblique impact loading, for various load angles, impact velocity and tube dimensions [3]. All the computer modeling of the above-mentioned study was conducted using the nonlinear finite element code ABAQUS/Explicit version 6.3. It was found that the mean load and energy absorption decrease significantly as the angle of applied load increases. Nevertheless, tapering a rectangular tube enhances its energy absorption capacity under oblique loading. The outcome of the study was design information for the use of straight and tapered thin-walled rectangular tubes as energy absorbers in applications where oblique impact loading is expected. According to various studies, cylinder internal pressure, projectile kinematic energy and the characteristics of a cylinder are effective factors in the damage caused by impact on under-pressure cylinders.

2. Problem analysis method

Ductile fracture criteria, such as the J-integral, the cohesive element method and the Gurson model, can be used for the modeling of damage in cylinders. Due to uncoupled governing equations, these criteria can be easily calibrated and implemented in a finite element code. Needing few coefficients and by applying accurate calibration, they are appropriate candidates for use in the simulation of impact problems. This is why they have been widely used in industrial practices [4]. All the above damage models assume that the damage model is uncoupled with the material constitutive equations. It means that the fracture criteria are checked at each step outside the loop of stress and strain calculations. When an accumulated damage indicator reaches a critical value in an element, it fails and completely loses its load-carrying capability.

Among damage models based on ductile fracture criteria, the Johnson-Cook (JC) model, which is formulated in the space of stress triaxiality and equivalent plastic strain, is capable of predicting realistic fracture patterns and, at the same time, correct residual velocities. Thus, this model is suitable for the prediction of fracture caused by impact problems [5]. Johnson and Cook developed a constitutive model to describe material properties under dynamic loading [6]. The von Mises yield criteria with the associated flow rule is used in this material model. Its isotropic hardening law includes the effects of strain rates and temperature rise. In conjunction with their material constitutive equation, Johnson and Cook also proposed a fracture criterion for dynamic loading problems. Similar to the material constitutive model, the fracture strain was assumed to be a function of stress triaxiality, strain rates, and temperature in an uncoupled form, defined by:

$$\bar{\sigma} = [A + B\varepsilon_{pl}^{n}]\left[1 + C\ln\left(\frac{\dot{\varepsilon}_{pl}}{\dot{\varepsilon}_0}\right)\right]\left[1 - \left(\frac{T - T_0}{T_m - T_0}\right)^{q}\right], \quad (1)$$

$$\varepsilon_f = \left[D_1 + D_2\exp\left(D_3\frac{\sigma_h}{\bar{\sigma}}\right)\right]\left[1 + D_4\ln\left(\frac{\dot{\varepsilon}_{pl}}{\dot{\varepsilon}_0}\right)\right]\left[1 + D_5\frac{T - T_0}{T_m - T_0}\right], \quad (2)$$

where $\bar{\sigma}$ is the equivalent stress; σ_h is hydrostatic pressure; ε_{pl} is the effective plastic strain; $\dot{\varepsilon}_{pl}$ and $\dot{\varepsilon}_0$ are the current and reference strain rates, respectively; T_m and T_0 are the melting and room temperature, respectively; and A, B, n, C, q and D_1,..., D_5 are material constants which need to be calibrated by experimental data. This model accounts for isotropic strain hardening, strain rate hardening and temperature softening in an uncoupled form.

The first term in the brackets in the right hand side of Eq. (2) has the same form as that proposed by Hancock and Mackenzie [8], and represents the fracture characteristics of a specimen under quasi-static loading conditions at room temperature. Since an exponential function was employed in the first term, Johnson and Cook implied that the fracture locus

could be represented by one continuous curve in the entire range, and the fracture strain decreases with the increasing stress triaxiality. In a general case, stress triaxiality is not constant but varies during a loading process. The stress triaxiality, defined as the ratio of the hydrostatic pressure to the equivalent stress, is commonly introduced in the literature to represent the stress state mentioned in Eq. (2). Note that hydrostatic pressure is the first invariant of the stress tensor, and the von Mises stress is the square root of the second invariant. Both invariants are independent of a coordinate system, and, thus, suitable for large plastic deformation. Impact problems involve large plastic deformation, high strain rates, and elevated temperature. Johnson and Cook assumed that damage accumulates in a linear way [7], i.e:

$$D = \int_0^{\varepsilon_{pl}} \frac{1}{\varepsilon_f} d\varepsilon_{pl}. \tag{3}$$

An element fails when D reaches unity, i.e. $D_{cr} = 1$. Due to high strain rates, heat generated by a large portion of plastic energy would not have sufficient time to escape to surrounding materials, which leads to temperature rise. Both strain rates and temperature clearly have an effect on the fracture characteristics of a specimen. According to the features that were counted on for Johnson-Cook's model and its availability in most finite element codes, it is used in the present paper.

3. Problem analysis

In this section, the modeling and analysis of CNG cylinders are presented and the results of the simulations are explained in detail.

3.1. Preliminary cylinder simulation

A 60-lit cylinder manufactured by the Faber Company in Italy is considered. The length of the cylindrical section is 668 mm. The inner and the outer diameters of the cylindrical section are 318 mm and 301.8 mm, respectively. The dimensions of the two end hemisphere used in the simulations are given in Figure 1. The cylinder is made of 4340 alloy steel, Johnson-Cook's material and damage model constants for this steel are listed in Table 1 [7].

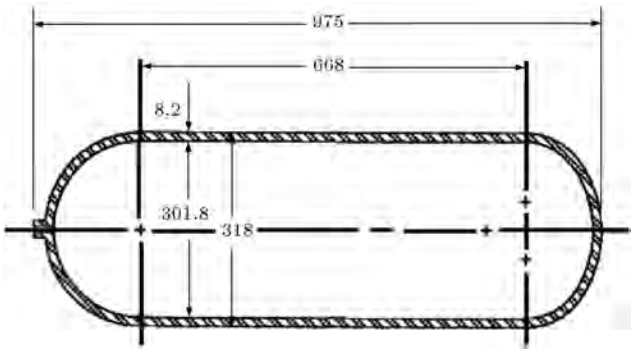

Figure 1. Scheme of the Faber all-steel cylinder in terms of mm [10].

The simulations are performed with the finite element software ABAQUS/Explicit [4], and the Johnson-Cook plasticity model and the Johnson-Cook damage model of ABAQUS/Explicit are used to describe the plastic constitutive material behavior and the damage initiation and propagation. For collision cases, side and normal directions, and for drop tests, side, oblique (45°) and normal directions, are considered. The CSA standard for a CNG cylinder is used to evaluate the impact damage and the ability to reuse the cylinder after collision. This association lists general guidelines for the value of the damage in the CNG cylinder in three levels. The levels are as follows [9].

- **Level 1**: Any scratch, gouge, or abrasion with a damage depth of less than, or equal to, 0.010 inch (0.25 mm). First level damage occurring on a cylinder is acceptable and it does not need to be repaired.
- **Level 2**: Any scratch, gouge, or abrasion with a damage depth of 0.011 to 0.050 inch (0.27 to 1.27 mm). Second level damage requires rework (either in the field or by the manufacturer), a more thorough evaluation or destruction of the cylinder, depending on severity.
- **Level 3**: Any scratch, gouge, or abrasion with a damage depth greater than 0.050 inch (1.27 mm). Third level damage is severe enough that the cylinder cannot be repaired and must be destroyed. All fire and chemical damage is Level 3, if it does not wash off [9].

According to the above levels, fine meshes were

Table 1. Material and damage model constants for 4340 alloy steel [7].

E (GPa)	ν	ρ (kg/m^3)	T_m(K)	T_0(K)	C_y(j/kg.K)
200	0.29	7830	1793	293	477
α(K^{-1})	A (MPa)	B (MPa)	n	C	m
0.000032	792	510	0.26	0.014	1.03
$\dot{\varepsilon}_0(S^{-1})$	D_1	D_2	D_3	D_4	D_5
1	0.05	3.44	-2.12	0.002	0.061

used up to the depth of 1.27 mm from the outer surface of the cylinder wall. Also, areas that are directly under impact have finer meshes where fracture is expected to occur. Relatively coarse meshes were used in the other part of the cylinder for increasing the speed of computing. Eight-node, linear brick elements with reduced integration were used. Failed elements were removed to illustrate the formation and growth of cracks. The kinematic contact constraint was prescribed at the impact interface, which allows the projectile to elastically rebound from the rigid wall at the end of the impact process. The friction coefficient between the front surface of the cylinder and the rigid walls is assumed to be 0.1. The duration of 20 ms is considered for all simulations. The results indicate that the damage during this period reaches a constant value.

3.2. Collision simulation of CNG cylinders

In this section, analysis of CNG cylinders under front and side collisions is investigated. The idea is to find out the effect collision direction has on the extent of damage in the cylinder. Due to the symmetry, only one-half of the cylinders was considered and the symmetric boundary conditions were applied at the plane of symmetry.

According to Figures 2 to 5, two cubes-shaped rigid surfaces are considered. One of them is the cylinder support during the accident, while the other is used as the impactor. To investigate the effect of internal pressure and the impactor collision velocity on the amount of damage to the cylinder, several cases were considered. The cases are listed in Table 2.

Pressure was uniformly applied to the inner surface of the cylinder. It should be mentioned that a speed of 120 km/h is the maximum velocity limit on highways.

Comparing the amount of damage on both sides of the cylinder shows that in the side collision, some areas in connection with the cylinder and the heads of the cylinder are damaged more than other parts (Figure 3). However, in a front impact, the middle parts of the heads of the cylinder have been damaged more than other areas and are, thus, considered critical areas (Figure 5).

Figure 2. Deformed model of the cylinder after side collision.

Figure 3. Critical area after side collision.

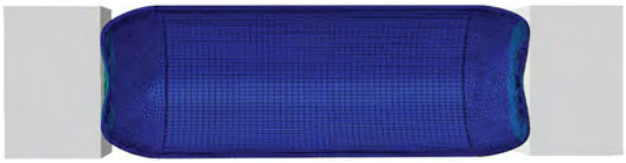

Figure 4. Deformed model of the cylinder after front collision.

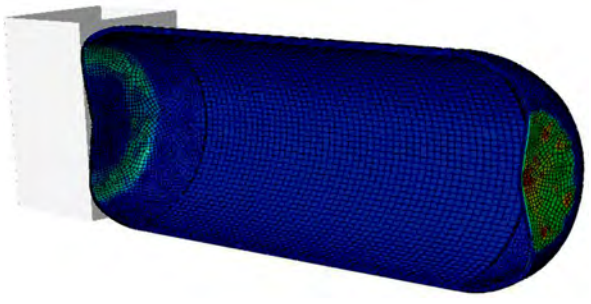

Figure 5. Critical area after front collision.

Table 2. Case studies for evaluation of damage on the CNG cylinder under collision.

Case studies	Pressure (bar)	Collision velocity (km/h)	Collision direction
Case 1	200	120	Side
Case 2	200	120	Front
Case 3	200	180	Side
Case 4	200	180	Front
Case 5	50	180	Side
Case 6	50	180	Front

By removing damaged elements from the damaged areas, in Figures 6 to 8, it is observed that for a side collision under working pressure (200 bars) and different velocities (i.e. cases 1 and 3), the depth of the damage in the cylinder wall is lower than the limits expressed in the CSA standard. Therefore, the cylinder can be used, if it is repaired again. However, under a pressure of 50 bars and at a velocity of 180 km/h (cases 5 and 6), the depth of the damage exceeds the acceptable amount, and the cylinder cannot be reused. In all states of front collision (cases 2, 4 and 6), the depth of damage on the cylinder wall exceeds the acceptable amount of damage and the cylinder cannot be reused. For cases under the pressure of 50 bars, the level of indentation depth is greater than similar cases under working pressure. This shows that by decreasing cylinder internal pressure, the amount of damage will be increased.

Figures 9 and 10 show that, initially, the damage in all cases has grown rapidly and, after a short time, it becomes flat. The results also indicate that for impacts in a front direction, the amount of damage was about twice in comparison with impacts in a side direction under the same conditions. Consequently, the number of omitted elements for impacts in a front direction is more. Also, it can be concluded that in cylinders with low pressure and higher velocity, the amount of accumulated damage for each specific direction is more.

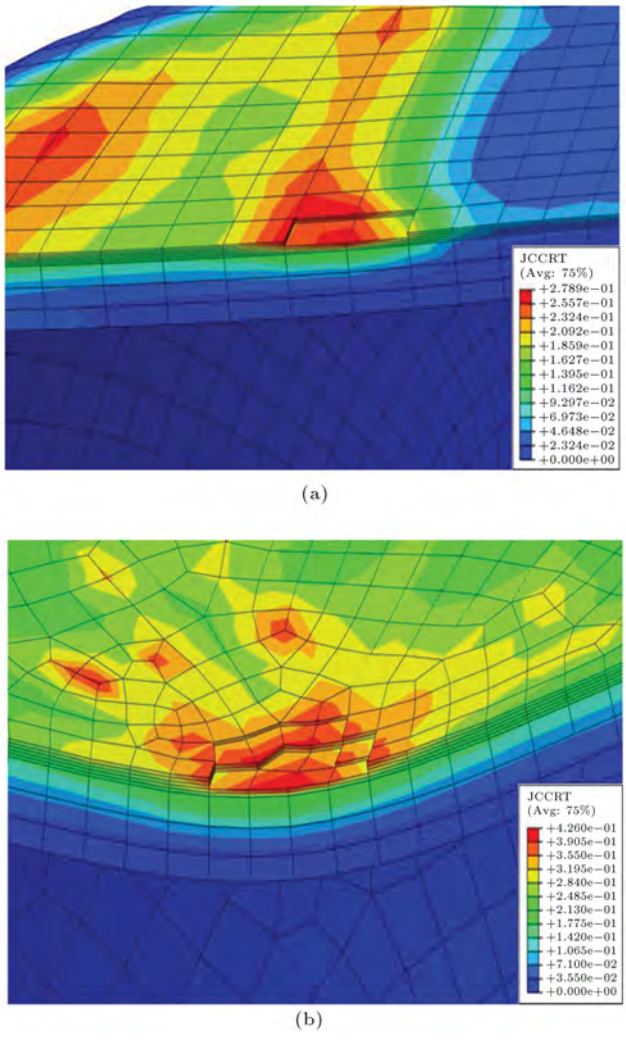

Figure 6. Damaged critical area in the collision for (a) case 1, and (b) case 2.

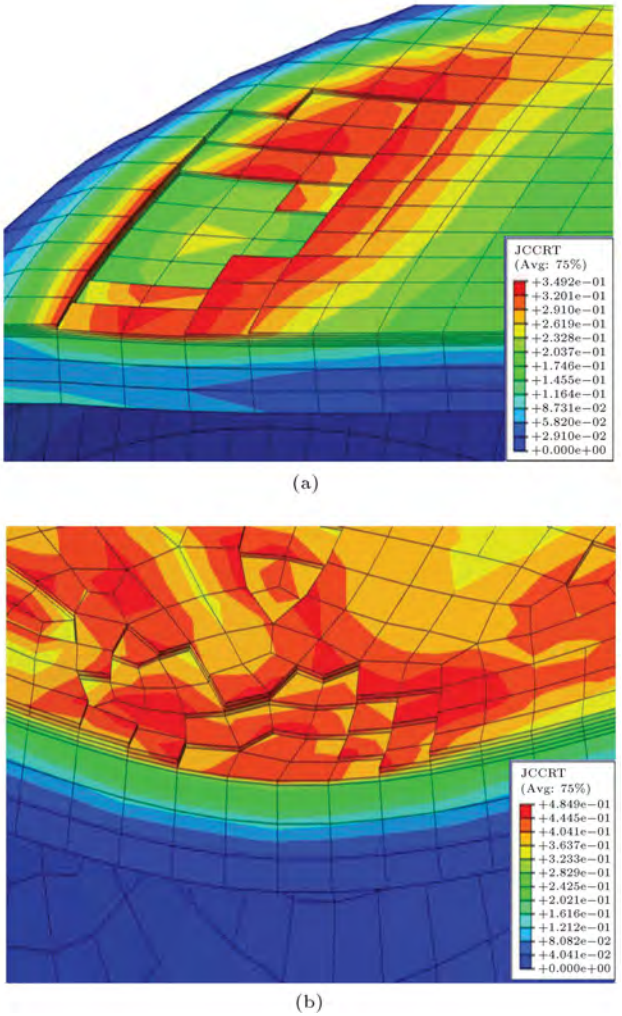

Figure 7. Damaged critical area in the collision for (a) case 3, and (b) case 4.

Comparing the history of equivalent plastic strain between critical points of collision in Figures 11 and 12, it shows that this quantity follows a trend very similar to the damage. Again, in the front direction, less pressure and higher colliding velocity creates more plastic strain. Figures 13 and 14 show the history of stress triaxiality for critical area in various directions of collision. A stress triaxiality of less than -0.5 is observed in most damaged areas. In the beginning the collision process, stress triaxiality rapidly decreases in the critical region for graphs corresponding to front collision. This indicates that for cases of higher

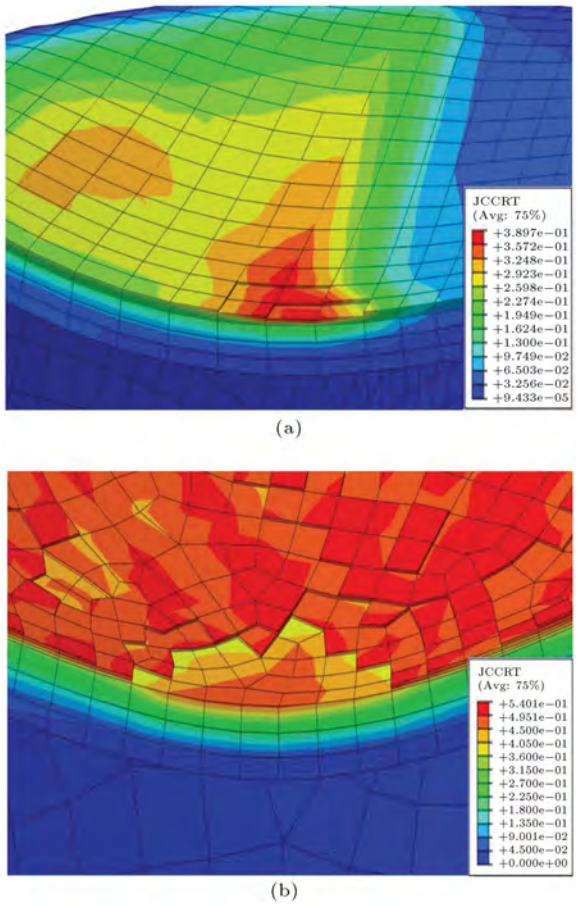

Figure 8. Damaged critical area in the collision for (a) case 5, and (b) case 6.

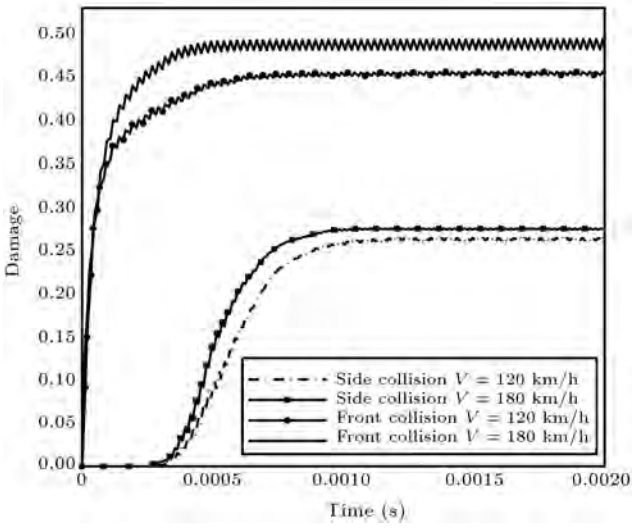

Figure 9. Damage growth rate at the critical damaged area for cases 1 to 4.

pressure, the bending is of more dominance in these areas.

Figure 15 shows a mesh study for cases 3 and 4 for a typical point in the critical area and for a point at a depth of 1.27 mm (maximum depth of damage).

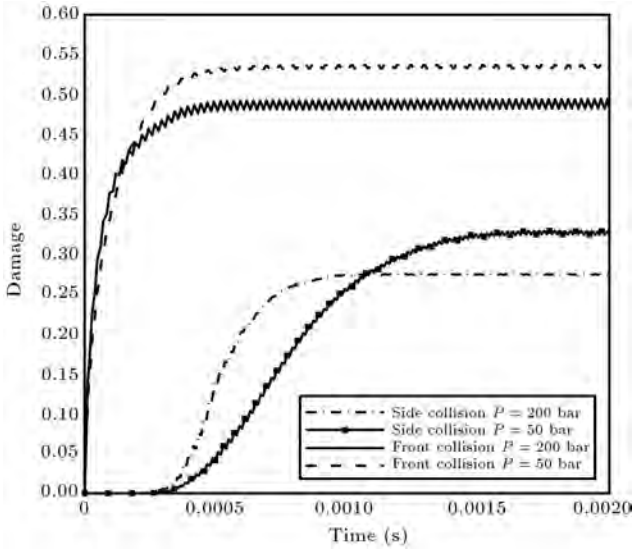

Figure 10. Damage growth rate at the critical damaged area for cases 3 to 6.

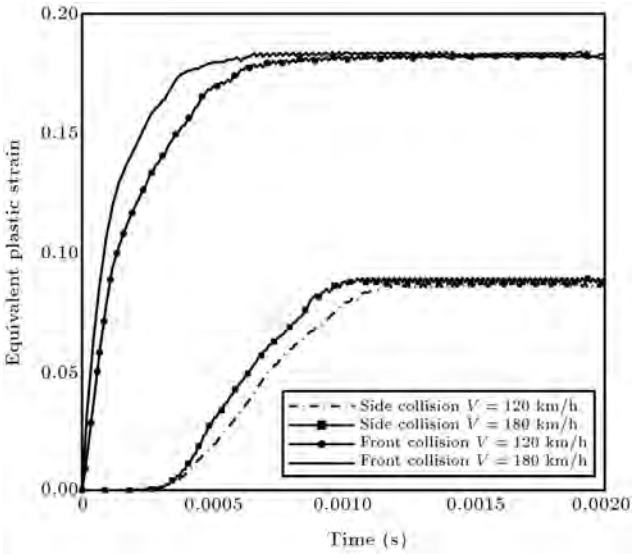

Figure 11. History of the equivalent plastic strain at the critical damaged area for cases 1 to 4.

The closeness of results to each other indicates that the obtained response does not depend on the mesh quality.

3.3. Drop test simulation of CNG cylinders

In this section, the analysis of the CNG cylinder for a drop test in side, oblique (45°) and normal directions is presented. According to Figures 16 to 19, in finite element models, the rigid surface of the cube-shaped cylinder has been considered as the colliding surface. In addition to different internal pressure, 25 and 6 m height of drop for each simulation direction have been applied as the initial velocity to the cylinder.

Figure 20 shows the critical area of the cylinder for side and oblique drop tests. Similar results were

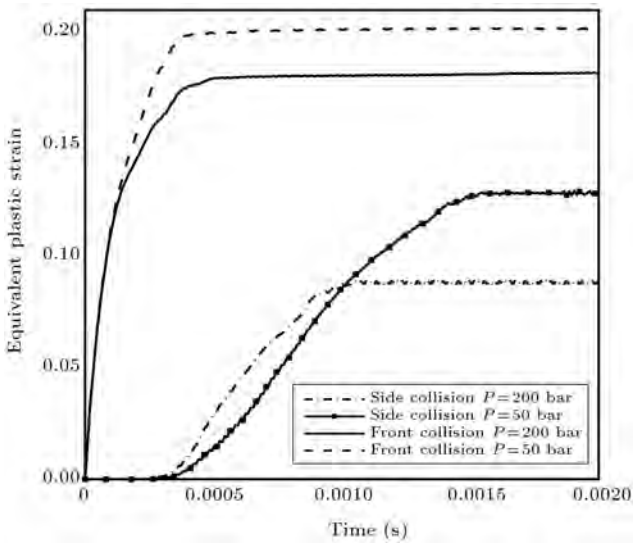

Figure 12. History of the equivalent plastic strain at the critical damaged area for cases 3 to 6.

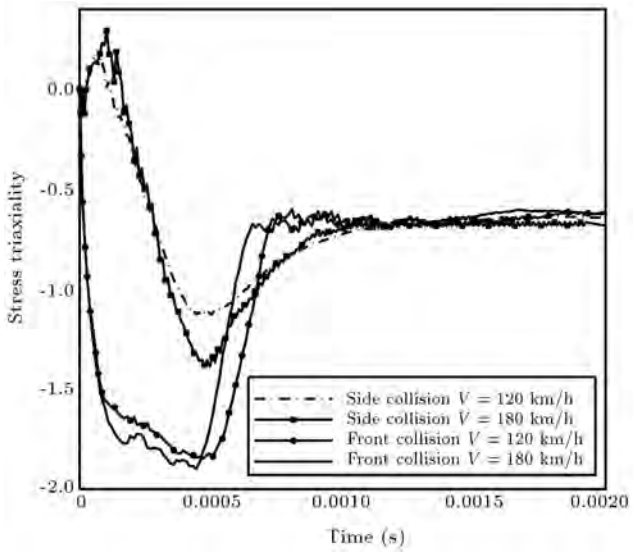

Figure 13. History stress triaxiality at the critical damaged area for cases 1 to 4.

obtained for the other side and oblique drop tests, which are not reported here for the sake of brevity. The results show that for all cases of side and oblique drop tests, the depth of damage does not go beyond the critical limit, and the cylinder can be used without any need for repair. It is noteworthy that by decreasing the internal pressure, the damage grows; however, its extent does not lead to the removal of any element from the cylinder.

According to Figures 21 and 22, when a cylinder with 200 bars pressure is dropped from different heights along a normal direction, the extent of the damage is somehow that after repair, the cylinder has the ability to be reused. Under conditions where the cylinder has an internal pressure of 50 bars and has fallen from a

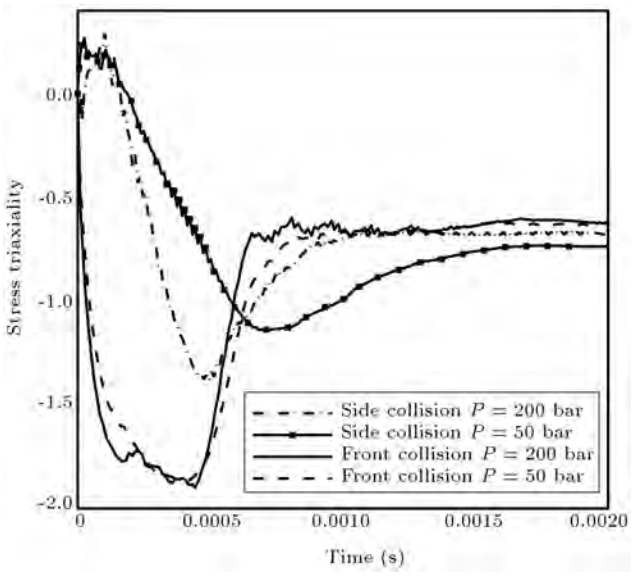

Figure 14. History of stress triaxiality at the critical damaged area for cases 3 to 6.

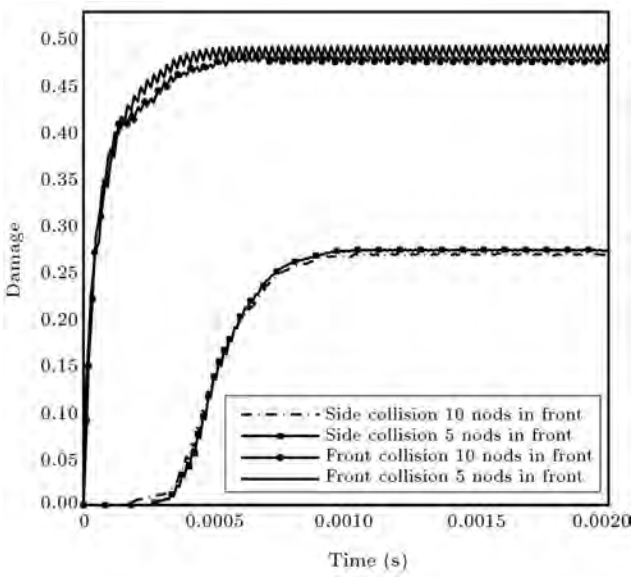

Figure 15. Damage rate in the collision for cases 3 and 4 (at 5 and 10 nodes from the outer surface of cylinder wall).

Figure 16. The deformed cylinder model after side drop test.

Figure 17. Critical area after side drop test.

Figure 18. The deformed cylinder model and critical area after oblique drop test.

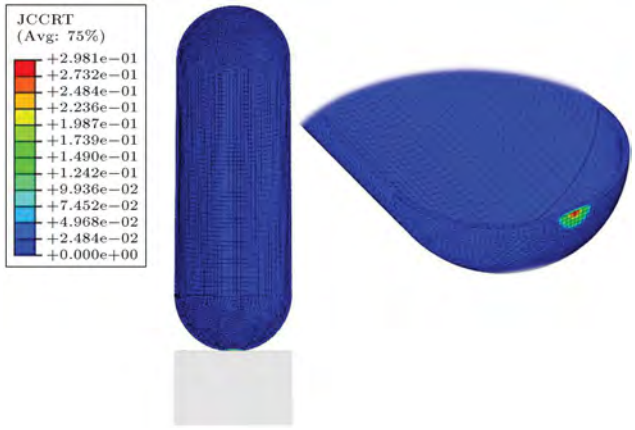

Figure 19. The deformed cylinder model and critical area after normal drop test.

height of 25 meters, the depth of the damage has gone beyond the critical value and the cylinder is not usable.

Figures 23 and 24 show the variation of damage versus time. The graphs indicate that the damage has grown rapidly and eventually reaches a constant value. Also, the amount of accumulated damage in a drop from a normal direction is more than in the others. By changing the angle of collision from the front to the side direction, the value of the damage is reduced. The amount of damage in normal drop increases more rapidly compared to the drop in other directions. The slope of the damage curves decrease by reducing the angle of collision. It can be concluded that by reducing

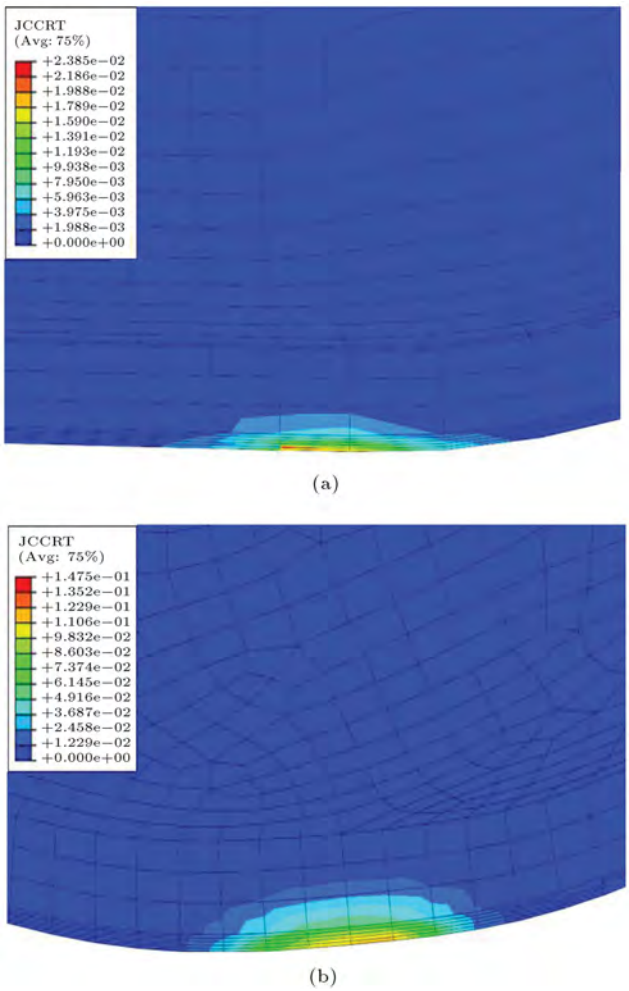

Figure 20. The critical area of the cylinder for (a) the side drop, and (b) oblique drop.

the pressure or increasing the height of the drop, the damage will be increased in all directions.

According to Figures 25 and 26, the equivalent plastic strain in the drop test follows the same trend as the damage growth. Here, for normal drop, less pressure and higher fall, higher plastic strain occurs. According to Figures 27 and 28, stress triaxiality is negative most of the time, which indicates that the damaged area is primarily under pressure. The drop in the stress triaxiality diagrams in the damaged area is affected by the pressure of bending, which is due to hitting the outer wall of the cylinder. It can be concluded that for a particular damaged area along a specific direction, at higher velocity and pressure, the drop in the graph of its corresponding triaxiality is more.

4. Conclusions

This paper examines the effect of direction and collision velocity, internal pressure and the height of fall on the damage in all-steel CNG cylinders using a damage

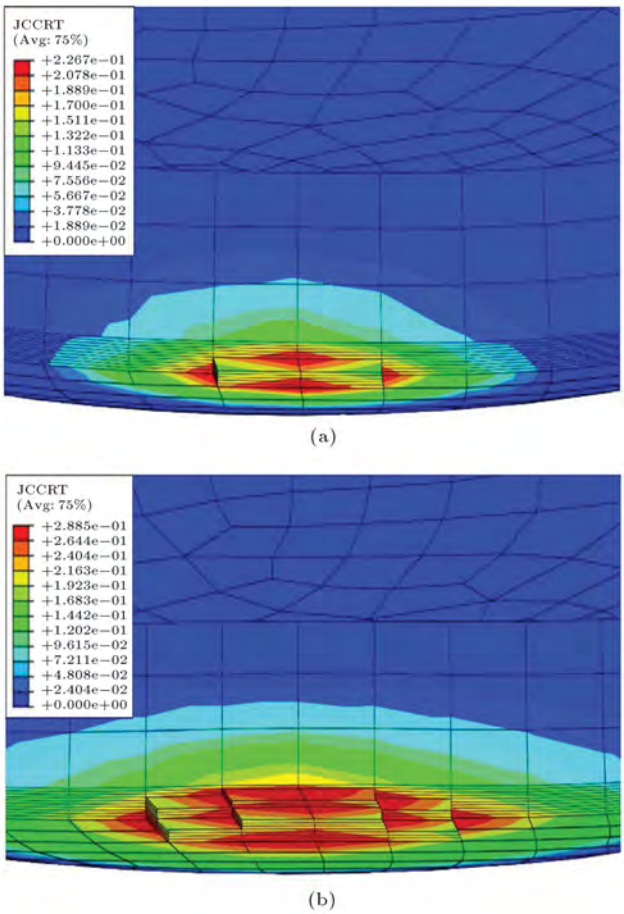

Figure 21. The critical area of the cylinder in normal drop for pressure of 200 bars: (a) Height of 6 m; and (b) height of 25 m.

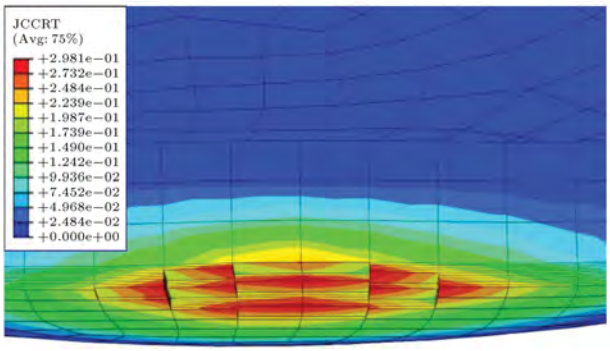

Figure 22. The critical area of the cylinder in normal drop for pressure of 50 bars and the height of 25 m.

mechanics approach. Two series of simulations were carried out on the CNG cylinders, namely, collision and drop test simulations. Reviewing the diagrams shows the maximum amount of damage occurred in drop from a normal direction, and by changing the drop direction from normal to side, the value and extent of damage will be reduced. With the removal of damaged elements and by comparing the depth of the damage in collision with the CSA standard, it was observed that in most

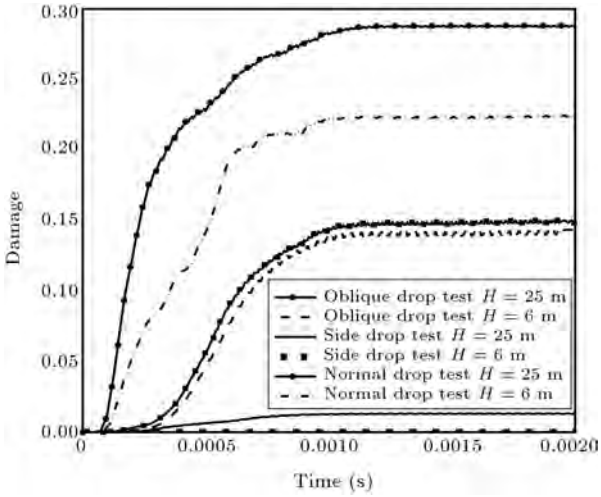

Figure 23. Damage growth rate in a typical point at damaged area (internal pressure of 200 bars).

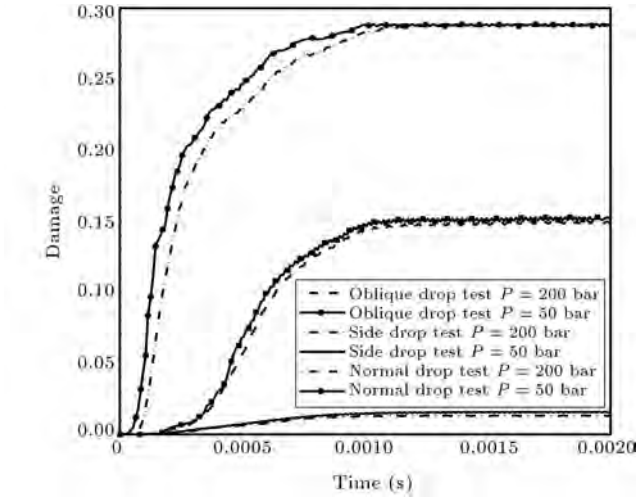

Figure 24. Damage growth rate in a typical point at damaged area (height = 25 m).

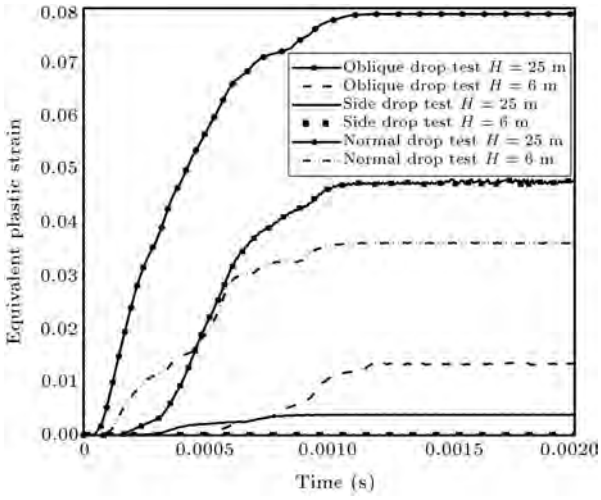

Figure 25. History of equivalent plastic strain at a typical point of damaged area (internal pressure = 200 bars).

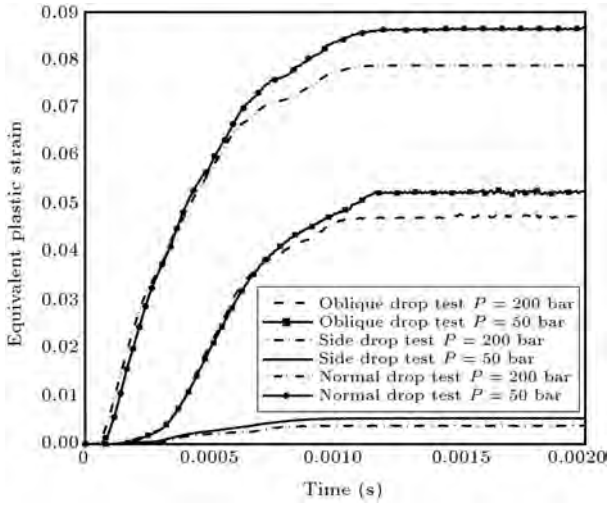

Figure 26. History of equivalent plastic strain at a typical point of damaged area (height = 25 m).

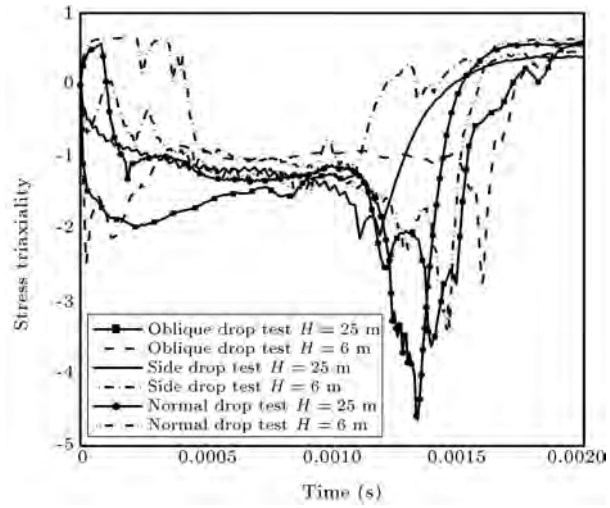

Figure 27. History of stress triaxiality at a typical point of damaged area (internal pressure = 200 bars).

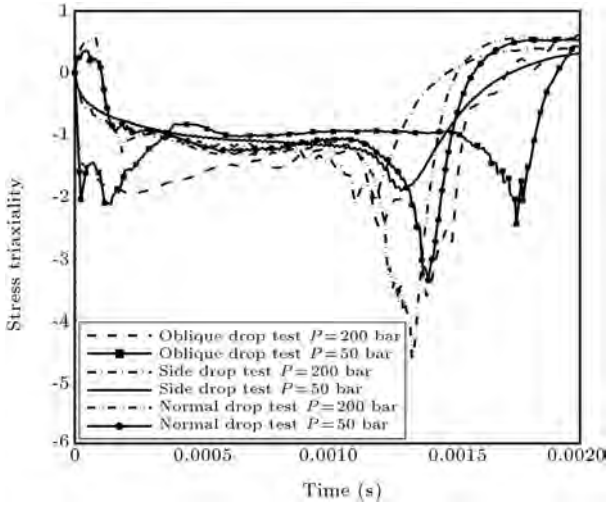

Figure 28. History of stress triaxiality at a typical point of damaged area (height = 25 m).

collision cases, and in a normal drop, the cylinder loses its ability to function.

In terms of side collision, the cylinder remains with no defect, and after repairing, it has the ability for reuse.

Results of simulation also showed that in all types of impact in cylinders with lower internal pressure the damage grows more than cylinders with higher internal pressure.

The results also revealed that in both side and front collisions, the cylinder's rear wall and the front head of the cylinder have more damage and are critical areas.

For a specific impact direction, by increasing collision velocity and the altitude of fall, or by decreasing cylinder pressure, the damage will also increase.

References

1. Becker, D.L., Burgess, D.M. and Lindquist, M.R. "Drop testing conducted to benchmark the shipping-port reactor pressure vessel package safety analysis", *Nucl. Eng. Des.*, **130**, pp. 133-145 (1991).
2. Rosenberg, Z., Mironi, J., Cohen, A. and Levy, P. "On the catastrophic failure of high-pressure vessels by projectile impact", *Int. J. Impact Eng.*, **15**, pp. 827-831 (1994).
3. Nagel, G.M. and Thambiratnam, D.P. "Dynamic simulation and energy absorption of tapered thin walled tubes under oblique impact loading", *Int. J. Impact Eng.*, **32**, pp. 1595-1620 (2006).
4. Teng, X. "High velocity impact fracture", PhD Thesis, Massachusetts Institute of Technology (2004).
5. Teng, X. and Wierzbicki, T. "Evaluation of six fracture models in high velocity perforation", *Eng. Fract. Mech.*, **73**, pp. 1653-1678 (2006).
6. Johnson, G.R. and Cook, W.H. "A constitutive model and data for metals subjected to large strains, high strain rates and high temperatures", in: *Proceedings of the Seventh International Symposium on Ballistics.*, Hague, Netherlands, pp. 541-47 (1983).
7. Johnson, G.R. and Cook, W.H. "Fracture characteristics of three metals subjected to various strains, strain rates, temperatures and pressures", *Eng. Fract. Mech.*, **21**(1), pp. 31-48 (1985).
8. Hancock, J.W. and Mackenzie, A.C. "On the mechanisms of ductile failure in high strength steels subjected to multi-axial stress-states", *J. Mech. Phys. Solids.*, **24**, pp. 147-169 (1976).
9. CSA America Inc. "CNG fuel system inspector study guide", National Energy Technology Laboratory, U.S. Department of Energy, DE-FC26-05NT42608 (2008).
10. T Ribarits, S.G. "Assessment of inspection criteria and techniques for recertification of natural gas vehicle (NGV) storage cylinders", M.Sc. Thesis, Mechanical Engineering Department, University of British Colombia (1983).

Biographies

Mohammad Yazdani Ariatapeh received BS and MS degrees in Mechanical Engineering from Sharif University of Technology, Iran, in 2008, and Isfahan University of Technology, Iran, in 2011, respectively. His research interests include solid design damage and fracture mechanics, finite element method and advanced design by computer.

Mohammad Mashayekhi received his PhD degree in Mechanical Engineering, in 2006, from Isfahan University of Technology, Iran, where he is currently Associate Professor of Mechanical Engineering. His research interests include damage mechanics, fracture mechanics, finite element method.

Saeed Ziaei-Rad received BS and MS degrees in Mechanical Engineering from Isfahan University of Technology, Isfahan, Iran in 1988 and 1990, respectively, and his PhD degree from the Department of Mechanical Engineering at Imperial College of Science and Technology, London, UK, in 1997. He is currently Professor and faculty member in the Mechanical Engineering Department of Isfahan University of Technology, Iran. He has many papers published in international journals and presented at conferences in his academic fields of interest.